Neuropharmacology 293 (2026) 110964

Contents lists available at ScienceDirect

Neuropharmacology

journal homepage: www.elsevier.com/locate/neuropharm

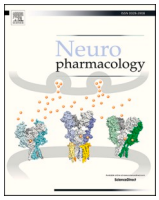

Single transient exposure to low-frequency low-intensity electrical stimulation produces ketamine-like effects in human iPSC-derived dopaminergic neurons via $Ca2^{+}$-dependent BDNF and mTOR signaling

Giulia Sofia Marcotto [a], Michela Borghetti [b], Jonida Bitraj [a], Laura Cavalleri [a], Mauro Serpelloni [b], Michele Zoli [c], Maurizio Memo [a], Emilio Sardini [b], Ginetta Collo [a,*]

[a] Department of Molecular and Translational Medicine, University of Brescia, Brescia, Italy
[b] Department of Information Engineering, University of Brescia, Brescia, Italy
[c] Department of Biomedical, Metabolic and Neural Sciences, University of Modena and Reggio Emilia, Modena, Italy

ARTICLE INFO

Keywords:
Structural plasticity
Exogenous electrical stimulation
Induced pluripotent stem cells
Cortisol
Stress
Major depressive disorders
Non-pharmacological approach

ABSTRACT

Electrical stimulation (ES) is emerging as a non-pharmacological neuromodulation strategy, but its direct impact on human dopaminergic neurons and its relationship to rapid-acting antidepressant mechanisms remain unclear. This study aimed to investigate whether brief biphasic low-frequency low-intensity (LF-LI) ES can induce structural and molecular plasticity in human induced pluripotent stem cell (iPSC)-derived mesencephalic dopaminergic neurons, identify the underlying signaling mechanisms, and evaluate its potential to rescue cortisol-induced impairments as in-vitro endocrine model of depression. iPSC-derived dopaminergic neurons were exposed to LF-LI ES using a custom culture-compatible stimulator, and structural plasticity was quantified three days later by computer-assisted morphometry. Pharmacological blockers, quantitative PCR and Western blot analyses were employed to assess calcium influx, brain-derived neurotrophic factor (BDNF)-TrkB-extracellular signal-regulated kinase (ERK)-mTOR signaling, and dopamine D3 auto-receptor roles in mediating LF-LI ES effects. A single 1h LF-LI ES session at 4 mA induced robust increases in maximal dendrite length, primary dendrite number, and soma area, comparable to 1 μM ketamine. LF-LI ES rapidly enhanced ERK and p70-S6K phosphorylation and required L-type voltage-gated calcium channels, TrkB and mTOR, as their inhibition prevented structural remodeling. LF-LI ES increased dopamine D3 auto-receptors mRNA, and its antagonism attenuated LF-LI ES-induced plasticity. In cortisol-treated neurons, LF-LI ES fully reversed dendritic hypotrophy and soma shrinkage. In conclusion, brief LF-LI ES elicits long-lasting, ketamine-like structural and molecular plasticity in human dopaminergic neurons and rescues stress hormone–induced impairments, supporting LF-LI ES-based neuromodulation approaches targeting dopaminergic circuits in major depressive disorder and treatment-resistant depression.

1. Introduction

Electrical activity is fundamental to neural function, enabling communication through synaptic interactions and direct electrical coupling (Balbinot et al., 2025). Neurons generate action potential via dynamic membrane potential changes mediated by voltage-gated ion channels. Exogenous electrical fields modulate neuronal function and plasticity, with therapeutic applications such as electro convulsive therapy (ECT), transcranial direct current stimulation (tDCS), transcranial alternate current stimulation (tACS), and deep brain stimulation (DBS) (Brunoni et al., 2016; Lozano et al., 2012). Major Depressive Disorders (MDD), a mood disorder characterized by episodes of low mood, anhedonia, negative emotions and hypercortisolemia, represents a leading global cause of disability (Malhi and Mann, 2018). Although pharmacological treatments targeting monoaminergic systems dominate approaches, nearly one-third of patients show treatment resistance (Fava, 2003). The discovery that sub-anesthetic doses of the N-methyl-D-aspartate (NMDA) receptor blocker ketamine produce rapid, sustained antidepressant effects in patients with treatment resistant depression (TRD) has shifted focus towards glutamatergic and

* Corresponding author. Department of Molecular and Translational Medicine, University of Brescia , Viale Europa 11, 25123, Brescia, Italy.
E-mail address: luigia.collo@unibs.it (G. Collo).

https://doi.org/10.1016/j.neuropharm.2026.110964
Received 17 February 2026; Received in revised form 26 March 2026; Accepted 2 April 2026
Available online 5 April 2026

brain-derived neurotrophic factor (BDNF)-dependent neurotransmission, implicitly bringing the focus on the defective neuroplasticity as a key pathogenic process underpinning TRD (Berman et al., 2000; Zarate et al., 2006). This single exposure studies were instrumental in establishing weekly or biweekly dosing therapeutic paradigms currently used in several 'ketamine' clinics (Strong and Kabbaj, 2018). Accordingly, a single low dose of ketamine infusion over 40-60 min induces antidepressant effects within hours that persist for up to two weeks, well beyond its pharmacokinetic presence (Berman et al., 2000). Robust, long lasting structural plasticity in neurons of brain corticolimbic circuits induced by 1h ketamine exposure was mediated via neurotrophic signaling, i.e., the extracellular signal-regulated kinase (ERK) and the mammalian target of rapamycin (mTOR) pathways (Cavalleri et al., 2018; Li et al., 2010). Thus, defective structural plasticity in glutamatergic telencephalic and dopaminergic (DA) mesolimbic circuits, along with mTOR dysregulation and BDNF down-regulation, characterizes mood disorders, whose symptoms were often reversed by rapid acting antidepressants and by electrotherapies, such as ECT, DBS, and tDCS (Cavalleri et al., 2018; Ousdal et al., 2022). Single or repeated ECT has been an effective treatment for MDD and TRD available in the clinic since 1938, yet its mechanisms remain incompletely understood (Ousdal et al., 2022; Sorri et al., 2018). Preclinical animal models demonstrate that repeated electro convulsive shock elicits widespread cell proliferation with neurogenesis in hippocampus and amygdala, and increases in dendrite length and spine density via BDNF- tropomyosin receptor kinase B (TrkB) pathway activation in telencephalic neurons, increases that correlate with cortical gray matter density signal in humans and increased hippocampal size (Dukart et al., 2014; Ousdal et al., 2022; Pirnia et al., 2016; Polyakova et al., 2015). The typical routine stimulation protocol includes high current amplitudes (800–900 mA) at approximately 5000 Hz in 0.3-1.0 ms pulses, inducing an electric field strength that exceeds the neural activation threshold by 1.8–2.9 times, affecting more than 94% of the brain volume at suprathreshold level, and delivering generalized seizures (Lee et al., 2016). This unselective paradigm is highly effective, but carries the risk of cognitive impairment, convulsion-associated adverse events, and gliosis by engaging all brain circuits and not those specifically involved in depression (Lee et al., 2016; Ousdal et al., 2022; Pirnia et al., 2016) A non-invasive and more selective brain stimulation technique with a radically different paradigm is tDCS, showing promise for TRD treatments with minor side effects (Brunoni et al., 2016; Ren et al., 2025). In TRD patients, tDCS applies low amplitude (1-2 mA) continuous (0 Hz) current in 30 min sessions through frontal scalp electrodes, generating electrical fields of 0.2-1.0 mV/cm, in the same range of 0.35-1.0 mV/cm neuronal activation thresholds, and engaging only sectors of cerebral cortex. These stimuli modulate neuronal excitability and synaptic plasticity, indirectly engaging distant brain structure via projecting circuits (Brunoni et al., 2016). Clinical trials demonstrate antidepressant efficacy with tDCS targeting dorsolateral prefrontal cortex, effects mediated through neuroplasticity mechanisms that includes increased BDNF signaling (Brunoni et al., 2016). Therapeutic effects in MDD were also reported in a well-designed study with 2 mA, 20 min session, low frequency (4-8 Hz) stimulation (Ren et al., 2025). The last paradigm, DBS, allows for direct electrical stimulation into highly restricted subcortical brain nuclei obtained via stereotaxic electrode placement in a neurosurgery setting. Widely used for Parkinson's disease (Limousin and Foltynie, 2019), DBS is also recommended for intractable TRD cases. Stimulation protocols implementing repeated sessions of low current (4-8 mA) with short pulse width (50–90 us) and high frequency (90-185 Hz) were developed for TRD, targeting subcortical structures such as subcallosal cingulate, nucleus accumbens, and medial forebrain bundle, all terminal fields of the ascending mesencephalic DA neurons (Figee et al., 2022; Lozano et al., 2012; Mayberg et al., 2005; Ramasubbu et al., 2018). Intriguingly, high frequency DBS would lead to local neuron inhibition via membrane depolarization block and enhancement of gamma-aminobutyric acid (GABA) transmission from afferent synapses (Herrington et al., 2016). In rodents DBS targeting nucleus accumbens led to complex long-term, indirect neurotrophic remodeling of connecting circuits, i.e., resulting in the enhancement of the 1-4 Hz spontaneous local field potential in the orbitofrontal cortex (McCracken and Grace, 2007) and increased mitochondrial function and BDNF expression in mesencephalic DA neurons (Li et al., 2023), all markers of neuroplasticity. These data further support the tenet that dysfunctional mesocorticolimbic DA system is a critical substrate of depression, particularly for anhedonia, a core diagnostic symptom of MDD and TRD (American Psychiatric Association, 2022; Nestler and Carlezon, 2006; Pizzagalli, 2014) and suggest that interventions promoting structural plasticity within this circuit may be therapeutic. Most of these paradigms only indirectly engage the mesocorticolimbic DA neurons located in the mesencephalon; however, evidence of direct effects of electrical stimulation (ES) on structural plasticity in human DA neurons is lacking. Using customized stimulation devices, several in vitro studies indicated that ES could be applied to cell cultures to gain insight into the molecular and cellular processes involved. Low-frequency (1-8 Hz)-low-intensity (0.1-4 mA), membrane activation threshold-like potential (0.5-1.8 mV/mm) ES were found to optimally induce a series of structural plasticity-relevant processes and molecular neurotrophic pathways activation in various neurons, neural progenitor cells (NPCs) and PC12 cells (Bertucci et al., 2019; Tominami et al., 2024; Zhu et al., 2019). Balanced biphasic waveforms ES was used in vitro to prevent charge accumulation and toxic byproduct formation, addressing integrity concerns when using human NPCs in cultures (Babona-Pilipos et al., 2012). Moreover, biphasic ES was shown to protect mouse olfactory bulb NPCs against growth factor-deprived apoptosis through BDNF- phosphoinositide 3-kinase (PI3K)/Akt pathway activation, enhancing cell survival and decreasing apoptotic rates (Wang et al., 2013). Likewise, exposure of NPCs to 0.53 or 1.83 V/m was associated with longer neurites, mature neuronal morphology, and increased βIII-Tubulin expression (Kobelt et al., 2014). In the present work, we investigated the effect of low-frequency low--intensity electrical stimulation (LF-LI ES) generated by a customized biphasic current stimulation system on human DA neurons differentiated from induced pluripotent stem cells (iPSCs). This differentiation protocol was previously used to study the structural plasticity effects of ketamine at exposure compatible with clinical antidepressant regimens, and to dissect out the receptors and intracellular pathways involved (Cavalleri et al., 2018). The present study evaluated whether LF-LI ES within clinically relevant amplitude (0.1-4.0 mA) and frequency (2 Hz), when applied transiently for 1h or 2h, can induce structural plasticity in mature human iPSC-derived DA neurons and compare them with the effects of rapid-acting ketamine. We hypothesized that LF-LI ES would promote dendritic outgrowth and structural plasticity through calcium-dependent activation of BDNF/TrkB - ERK - mTOR pathways. Furthermore, we investigated whether LF-LI ES can reverse cortisol-induced dendritic hypotrophy in an in vitro translational depression model, providing functional evidence for potential antidepressant-like effects (Cavalleri et al., 2024). This translational approach would clarify molecular substrates of this LF-LI ES neuromodulation, identify convergent mechanisms with established interventions, and may inform development and optimization of new technical solutions in humans for mood disorders characterized by DA dysfunction and impaired structural plasticity.

2. Materials and methods

2.1. Pharmacological agents

LY294002 (10 μM), rapamycin (0.02 μM), SB277011-A (0.05 μM), K252a (0.2 μM), PP2 (10 μM), hydrocortisone (cortisol) (50 μM), 2-APB (50 μM) (Tocris Bioscience) Nifedipine (5 μM) (Abcam), and Ketamine (1 μM) (ACME) were used in this study. Ketamine was dissolved in water; LY294002, rapamycin, SB277011-A, K252a, PP2, hydrocortisone, 2-APB and Nifedipine were dissolved in dimethyl sulfoxide. The

concentration of LY294002, ketamine, rapamycin, SB277011A, K252a, PP2, and hydrocortisone were established in our previous publications (Cavalleri et al. 2018, 2024; Collo et al., 2018). The concentrations of 2-ABP and Nifedipine were derived from Maruyama et al. (1997) and Wang et al. (2023), respectively. For each control treatment, the vehicle was prepared with the respective dilution of dimethyl sulfoxide. Additional information about pharmacological agents is available in Supplementary Table 1.

2.2. Low-frequency low-intensity electrical stimulation system

Cells were cultured in a standard 6-well plate and stimulated using electrodes integrated into a modified C-Dish lid (IonOptix), specifically adapted for this application by interconnecting 3 ml wells. Each well was endowed with two electrodes separated by a space of 23.4 mm where the cell culture was located. The electrical current stimulation was provided by a custom-designed system, as illustrated in Fig. 1. The stimulator is controlled via an interface developed in LabVIEW. A voltage signal replicating the desired current waveform is generated by the software and provided as an output through channel A0–A2 of a National Instruments NI6001 board. Each generated voltage signal is converted into current by the stimulator (84 mm × 95.5 mm x 50 mm), through dedicated circuit (Fig. 1A, insert in the middle) included in the stimulator, which drives a pair of wells. The NI6001 board also features a current monitoring function of I1–I3, enabling verification of the actual stimulation delivered to each well pair. The conditioning circuit is powered by an MB102 breadboard power supply module set to 5 V (53 mm × 27 mm). In this study, a biphasic rectangular waveform was used to prevent the accumulation of unrecoverable charge known to negatively affect cellular functions (Babona-Pilipos et al., 2012; Wang et al., 2013). The stimulation parameters were set as indicated by literature (Leondopulos et al., 2012; Tang-Schomer, 2018) to a frequency of 2 Hz and a variable current amplitude 1.0 - 4.0 mA that delivered a maximal local field estimated to be of 0.65 mV/cm. Each pulse (Ton1 and Ton2) lasted 50 ms, with a 1 ms interphase between the negative and positive phases. The resistance measured at the immersed electrode level was 380 Ohm at 1 kHz.

2.3. iPSCs culture and maintenance

The healthy control line 244CP-F3 was previously generated and fully characterized in our laboratory (Collo et al., 2018). Dermal biopsy

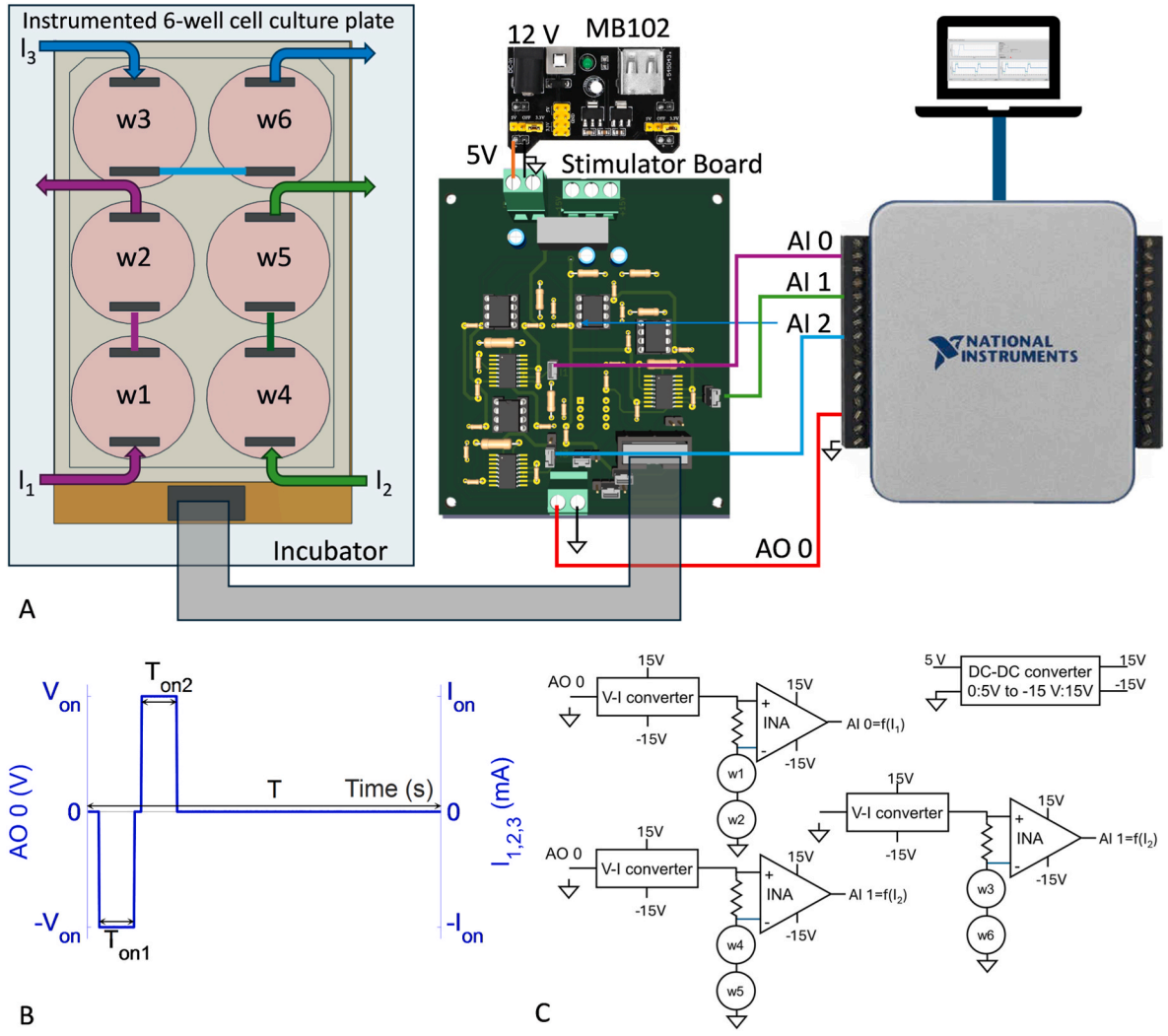

Fig. 1. Low-frequency low-intensity electrical stimulation system. (A) Schematic representation of the custom electrical stimulation system for 6-well cell culture plates. A biphasic rectangular voltage waveform, generated via LabVIEW at AO 0 V output of the NI6001 DAQ board, is converted into current by the stimulator board, composed of three dedicated circuits, each serving two wells. Current monitoring is performed via channels AI 0, AI 1, and AI 2. The system is powered by a 5 V MB102 breadboard power supply module. (B) Biphasic rectangular voltage and resulting current waveform use for the cell stimulation (C) Schematic block diagram of the analog stimulator board.

of a 40 years old Caucasian female donor was obtained with informed consent and approval from the local ethics committee (CEIOC—Fatebenefratelli Hospital "San Giovanni di Dio," Brescia, Italy, 44/2001 and 39/2005). iPSCs were cultured on Biolaminin-coated plates (BioLamina AB) and mTeSRTM1 medium (StemCell Technologies) supplemented with ROCK inhibitor 10 μM.

2.4. Differentiation of iPSCs into DA neurons

iPSCs were differentiated into floorplate-derived DA neurons via dual-SMAD inhibition and floor plate patterning, following previous published protocol (Fedele et al., 2017; Kriks et al., 2011) with minor modifications. iPSCs were dissociated using Accutase™ (StemCell Technologies) and plated on Biolaminin-coated plates in knockout serum replacement medium supplemented with LDN193189 (0.1 μM, Miltenyi Biotec), SB431542 (10 μM, Tocris Bioscience), SHHC25II (0.1 μg/ml, Peprotech), purmorphamine (2 μM, Peprotech), fibroblast growth factor 8 (FGF8 0.1 μg/ml, Peprotech), and CHIR99021 (3 μM, Miltenyi Biotec). From day 5, medium was gradually switched to N2. On day 11, cultures were transitioned to Neurobasal/B27 containing CHIR99021, BDNF (20 ng/ml, Peprotech), Ascorbic acid (AA 0.2 mM, Sigma-Aldrich), Adenosine-3′,5′-cyclic monophosphate (cAMP 0.5 mM, Sigma-Aldrich), transforming growth factor type β3 (TGF-β3 1 ng/ml, Peprotech), glial cell line-derived neurotrophic factor (GDNF 20 ng/ml, Peprotech), and DAPT (10 nM, Tocris Bioscience). On day 21, cells were replated onto poly-DL-ornithine/fibronectin/laminin-coated plates (Sigma-Aldrich), and co-cultured with primary mouse cortical astrocytes. LF-LI ES and drug treatments started on day 30. The full characterization of differentiated DA neurons from 244CP-F3 line was previously described (Collo et al., 2018). Quantitative PCR (qPCR) performed at day 30 and 60 of differentiation showed no changes in the expression of tyrosine hydroxylase (TH), G protein-coupled inwardly rectifying potassium channel 2 (GIRK2), nuclear receptor related 1 protein (NURR1), and dopamine D2 receptor (DA-D2R) supporting the use of DA neurons at 30 days of differentiation in the following experiments Supplementary Figure S1.

2.5. Immunocytochemistry assays

Cultures were fixed with Antigenfix (DiaPath) for 15 min at room temperature (RT), then permeabilized with 0.2% Triton X-100 (Sigma-Aldrich), 1% normal goat serum (NGS; Jackson ImmunoResearch), and 5% bovine serum albumin (BSA, Sigma-Aldrich) for 45 min at RT. Samples were incubated overnight (ON) at 4 °C with mouse monoclonal anti-TH antibody (Santa Cruz Biotech), followed by 1h incubation with biotinylated goat anti-mouse secondary antibody (Jackson ImmunoResearch). Detection was performed using an avidin–biotin–HRP complex (Vector Labs), and 3,3′diaminobenzidine (DAB; Sigma-Aldrich) was add for 5 min to develop the signal. Samples were imaged using an Olympus IX51 microscope (Olympus). Each experiment was performed in duplicate. Additional information about antibodies is available in Supplementary Table 2 and Supplementary Table 3.

2.6. Computer-assisted morphometric analysis

Digital images were acquired using an Olympus IX51 microscope equipped with an Olympus digital camera and connected to a PC. Morphometric analyses were performed by a blinded examiner on digitized images using ImageJ. Structural plasticity of DA neurons was assessed based on three morphological parameters: (i) maximal dendrite length, (ii) number of primary dendrites, and (iii) soma area as previously described (Collo et al., 2018) Significant changes in these endpoints, evaluated in >30 neurons per group, were considered indicative of structural plasticity alterations (Schmidt et al., 1996). Two coverslips per treatment group were analysed, yielding >30 frames per coverslip and from 30 to 100 neuron measurements. Each experiment was performed in duplicate.

2.7. RNA isolation and quantitative reverse transcription PCR

Total RNA was extracted using the NucleoSpin® kit (Macherey-Nagel) according to the manufacturer's protocol. RNA concentration and purity were assessed with a NanoDrop® 1000 spectrophotometer (Thermo Fisher Scientific). 1 μg of RNA was reverse-transcribed into cDNA using the ImProm-II™ Reverse Transcription System (Promega). qPCR was performed in duplicate, each in technical triplicate, using iTaq™ Universal SYBR® Green Supermix (Bio-Rad) on a ViiA™ 7 Real-Time PCR System (Applied Biosystems). Reactions included 10 ng of cDNA and 200 nM of each primer in a 10 μl final volume. Cycling conditions were 95 °C for 5 min, followed by 40 cycles at 95 °C for 35 s and 60 °C for 1 min. Relative gene expression was calculated using the 2^−ΔΔCt method and normalized to Glyceraldehyde-3-phosphate dehydrogenase (GAPDH), which remained stable under experimental conditions. Primer sequences are listed in Supplementary Table 4.

2.8. Western blotting

Western blotting was performed at multiple time points (1–5 min) following LF-LI ES. At each time point, neuronal cultures were rinsed with ice-cold PBS and lysed in radioimmunoprecipitation assay (RIPA) buffer containing protease inhibitors (Roche Diagnostics) for 30 min on ice. Lysates were homogenized using a probe sonicator. Protein concentration was determined using the Pierce™ BCA Protein Assay Kit (Thermo Fisher Scientific). Equal amounts of protein (10 μg) were resolved on 10% sodium dodecyl sulfatepolyacrylamide gel electrophoresis or on NuPAGE™ 4–12% Bis-Tris gels (Invitrogen) and transferred to polyvinylidene difluoride membranes (Immobilon-P; Millipore). Membranes were blocked with 5% BSA and 0.1% Tween20 (Sigma-Aldrich) and incubated overnight at 4 °C with primary antibodies: anti-phosphorylated ERK (p-ERK) mouse mAb (1:2000), anti-ERK mouse mAb (1:2000) (Santa Cruz Biotechnology), anti-p-p70-S6 Kinase1 (p-p70-S6K) mouse mAb (1:1000), anti-p70-S6 Kinase1 (p70-S6K) rabbit mAb (1:2000) (Cell Signaling Technology), and anti-α-Tubulin mouse mAb (1:20000) (Sigma-Aldrich). After washing, membranes were incubated with HRP-conjugated goat anti-rabbit or anti-mouse secondary antibodies (Santa Cruz Biotechnology) for 1h at RT. Signal detection was performed using an enhanced chemiluminescence substrate (ECL, LiteAblot Extend; EuroClone). Bands were visualized on film or using a G:Box Chemi XT Imaging system (Syngene, UK) and quantified by densitometric analysis using Gel-Pro Analyzer software (Media Cybernetics). p-ERK and p-p70-S6K signals were normalized to total ERK and p70-S6K, respectively, and then to α-Tubulin levels from the same sample. Additional information about antibodies is available in Supplementary Table 2 and Supplementary Table 3.

2.9. Statistical analysis

Each experiment was repeated at least twice independently. For morphometric analyses, individual data points represent single neuron measurements obtained from two coverslips per treatment group within a technical replicate; each experiment was replicated at least twice. Data are presented as mean ± standard error of the mean (SEM), unless otherwise indicated. Statistical analysis was performed using one-way or two-way ANOVA, followed by Bonferroni's post hoc test for multiple comparisons, or Friedman test. In cases where only two groups were compared, data were analysed using Student's *t*-test. All statistical analyses were performed using GraphPad Prism v10.0 (GraphPad Software, San Diego, CA, USA). Statistical significance was set at $P < 0.05$.

3. Results

3.1. Effects of single low frequency-low intensity electrical stimulation exposure on neural plasticity of human DA neurons differentiated from iPSCs

At day 30 of differentiation, corresponding to a postmitotic stage suitable for functional assays, human DA neurons were exposed to LF-LI ES for either 1h or 2h period using different amplitudes for the biphasic current waveform: 0, 1, 2, or 4 mA (Fig. 2A). Parallel wells were exposed to either vehicle (V) or to ketamine (K), a rapid acting, clinically effective antidepressant known to induce axonal growth and soma size expansion in human and rodent DA neurons with 1h exposure (Cavalleri et al., 2018). Following the previously established protocol (Cavalleri

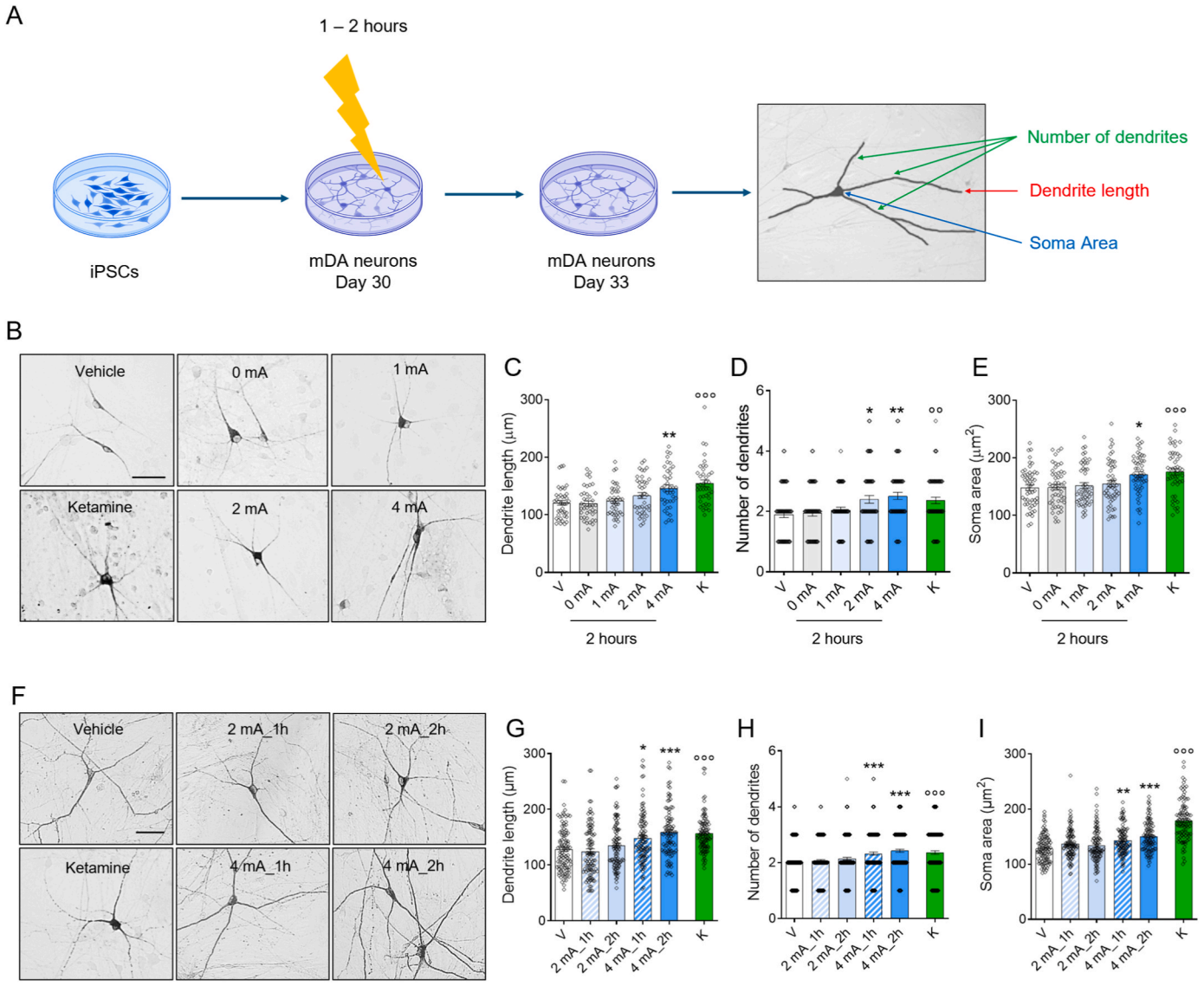

Fig. 2. Amplitude- and time-response effects of single low-frequency low-intensity electrical stimulation on structural plasticity. (A) Schematic representation of human dopaminergic (DA) neurons differentiation and single low-frequency low-intensity electrical stimulation (LF-LI ES) timeline. The inset in the right represents the image analysis markers used as outcome. (B) Representative images of human DA neurons after exposure to a single 2h LF-LI ES by biphasic electrical currents at various amplitudes (0, 1, 2, or 4 mA for 2h) or ketamine (K) (1 µM for 1h) used as active control test, vs. vehicle (V). Scale bar: 50 µm. (C-E) Quantification and statistical analysis of the effects of LF-LI ES conditions vs V using one-way ANOVA of (C) maximal dendrite length [$F(4,195) = 5.8$, $P < 0.001$], (D) number of primary dendrites [$F(4,295) = 6.25$, $P < 0.001$] (full frequency distribution of dendrite counts per neuron shown in Supplementary Figure S4A), and (E) soma area [$F(4,245) = 3,54$, $P < 0.001$] in human DA neurons. Post-hoc t-tests were performed to assess the effect of K vs V of (C) maximal dendrite length [$t(78) = 4.68$, $p < 0.001$], (D) number of primary dendrites [$t(118) = 3.04$, $p < 0.01$], and (E) soma area [$t(98) = 3.84$, $p < 0.001$] in human DA neurons. Since exposure to LF-LI ES at 0 mA did not induce detectable changes in structural plasticity measures, this condition was not included in subsequent experiments. (F) Representative images of human DA neurons following exposure to vehicle or LF-LI ES by biphasic electrical current with different stimulation parameters (2 mA or 4 mA for 1h or 2h), or K (1 µM for 1h) used as active control test, vs. V. Scale bar: 50 µm. (G-I) Quantification and statistical analysis of the effects of LF-LI ES conditions vs V using one-way ANOVA of (G) maximal dendrite length [$F(4,460) = 9.81$, $P < 0.001$], (H) number of primary dendrites [$F(4,995) = 11.77$, $P < 0.001$] (full frequency distribution of dendrite counts per neuron shown in Supplementary Figure S4B), and (I) soma area [$F(4,495) = 10.08$, $P < 0.001$] in human DA neurons. Post-hoc t-tests were performed to assess the effect of K vs V of (G) maximal dendrite length [$t(198) = 5.44$, $p < 0.001$], (H) number of primary dendrites [$t(398) = 4.49$, $p < 0.001$], and (I) soma area [$t(198) = 11.55$, $p < 0.001$] in human DA neurons. Individual data points represent single neuron measurements from two coverslips per group (technical replicate); each experiment was repeated at least twice independently. Data are presented as mean ± SEM. Statistical significance: ***$P < 0.001$; **$P < 0.01$; *$P < 0.05$ vs. V (post-hoc Bonferroni test); °°°$P < 0.001$; °°$P < 0.01$; °$P < 0.05$ vs. V (post-hoc *t*-test).

et al., 2018), 3 days after the LF-LI ES session, cultures were fixed and immunostained with an anti- TH antibody to identify human DA neurons. Morphological parameters, including dendrite length, number of primary dendrites, and soma area, were quantitatively analysed to assess the effects of LF-LI ES on structural plasticity. Morphological analysis showed that 2h exposure to LF-LI ES produced dose-dependent significant increases of maximal dendrite length, dendrite number and soma area with the strongest effect observed at 4 mA, the maximal dendrite length showing increases also with 2 mA. These effects were similar to those produced by ketamine. (Fig. 2B–E). Repeated exposures to the same current amplitudes for 3 days delivered an enhanced structural plasticity of the same magnitude, suggesting that a single exposure can already reach a structural plasticity plateau (Supplementary Figure S3). In a second set of experiments human DA neurons were exposed to 2 mA or 4 mA LF-LI ES for 1h or 2h period. Morphological analysis performed 3 days after exposure showed that 4 mA LF-LI ES for 1h was sufficient to produce a significant increase of maximal dendrite length, dendrite number and soma area (Fig. 2F–I). Therefore, the stimulation conditions of 4 mA for 1h were selected for the next experiments aimed to study gene expression and molecular pathways engagement in the LF-LI ES -dependent neuroplasticity process. Since the same effects were observed in DA neurons at 60 days of differentiation (Supplementary Figure S2), all subsequent experiments were performed using 30-day differentiated DA neurons as a standardised and reproducible cellular model.

3.2. *Low frequency-low intensity electrical stimulation promotes structural plasticity via extracellular Ca2+ signalling*

The role of extracellular and intracellular Ca2+ release in neuronal plasticity induced by LF-LI ES was investigated at day 30 of differentiation of human DA neurons with the L-type Ca2+ channel extracellular blocker Nifedipine and the intracellular blocker IP3 receptor agonist 2-APB added to the culture 20 min before 1h exposure to LF-LI ES. (Fig. 3A and B). The morphological analysis of human DA neurons performed 3 days later indicated that the L-type Ca2+ extracellular blocker Nifedipine significantly prevents structural plasticity changes induced by 4 mA for 1 h LF-LI ES. In contrast, no significant effects were observed with the intracellular Ca2+ channel antagonist 2-APB (Fig. 3C–E), suggesting that extracellular Ca2+ via voltage-gated calcium channels (VGCCs) plays an important role in triggering the LF-LI ES-mediated dendrite outgrowth as previously described (Morton et al., 2013), a mechanism also engaged by ketamine (Li et al., 2010).

3.3. *BDNF-TrkB-ERK-mTOR intracellular signalling mediates structural plasticity induced by low frequency-low intensity electrical stimulation*

In the present experiment aimed to profile the acute response of intracellular pathways to LF-LI ES exposure, human DA neuronal cultures at day 30 of differentiation were exposed to 4 mA LF-LI ES for 1, 2, or 5 min, timepoints selected to capture rapid kinase phosphorylation

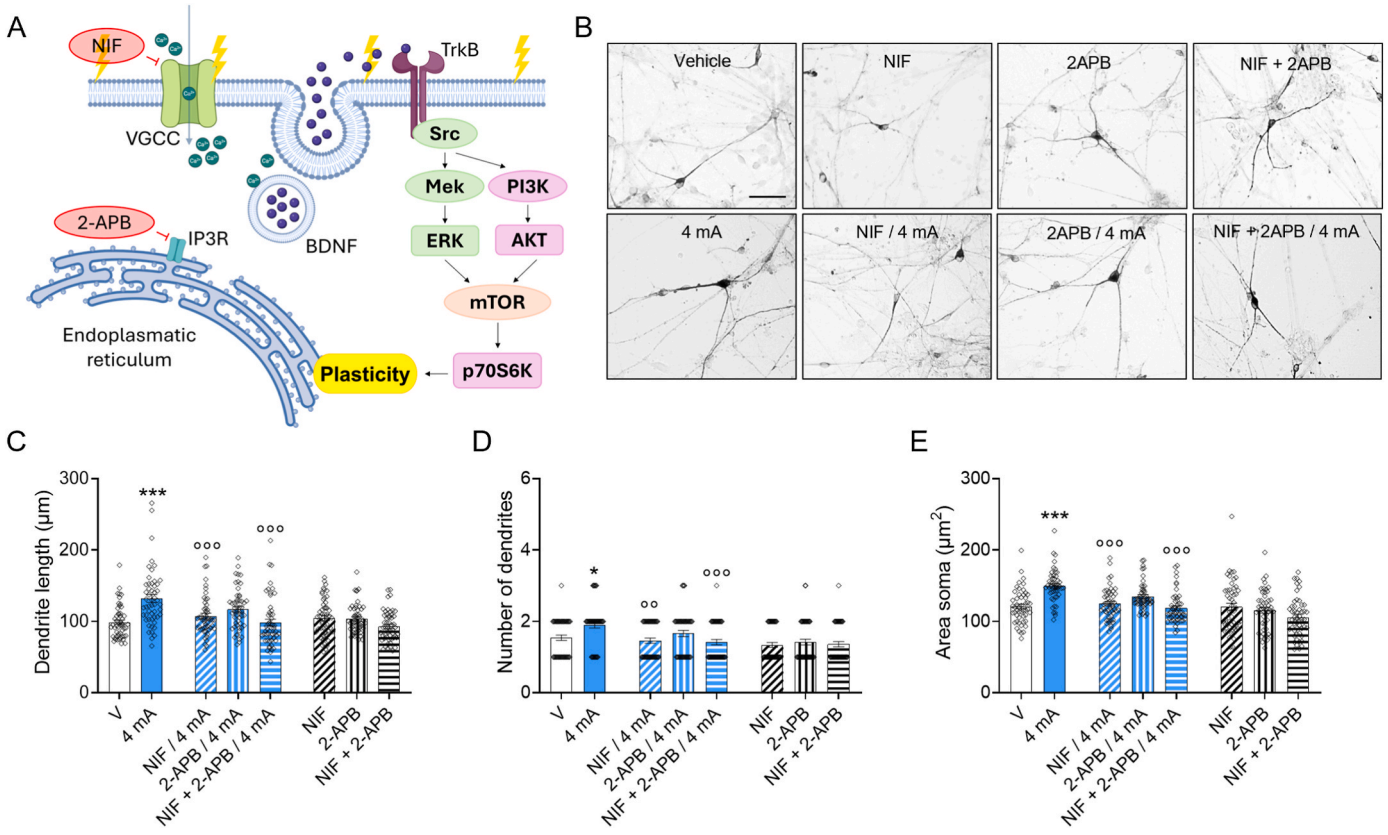

Fig. 3. Role of calcium signaling in neural plasticity induced by low-frequency low-intensity electrical stimulation. (A) Schematic representation of the intracellular and extracellular Ca^{2+} activated pathways and the site of actions of the Ca^{2+} channel blockers used to explore their involvement in LF-LI ES-dependent neuroplasticity. (B) Representative images showing morphological changes in human DA neurons exposed to a single LF-LI ES of 4 mA for 1h and pretreated for 20 min with Nifedipine (NIF), 2-APB or NIF+2-APB. Scale bar: 50 µm. (C-E) Quantification and statistical analysis using two-way ANOVA of (C) maximal dendrite length [interaction: $F(3,408) = 6.00$, $P < 0.001$; treatment factor: $F(1,408) = 23.23$, $P < 0.001$; inhibition factor: $F(3,408) = 8.98$, $P < 0.001$], (D) number of primary dendrites [interaction: $F(3,392) = 1.45$, $P < 0.23$ ns; treatment factor: $F(1,392) = 12.46$, $P < 0.001$; inhibition factor: $F(3,392) = 7.81$, $P < 0.001$] (full frequency distribution of dendrite counts per neuron shown in Supplementary Figure S4C), and (E) soma area [interaction: $F(3,392) = 4.21$, $P < 0.01$; treatment factor: $F(1,392) = 40.90$, $P < 0.001$; inhibition factor: $F(3,392) = 13.83$, $P < 0.001$] in human DA neurons. Individual data points represent single neuron measurements from two coverslips per group (technical replicate); each experiment was repeated at least twice independently. Data are presented as mean ± SEM. Statistical significance: ***$P < 0.001$; **$P < 0.01$; *$P < 0.05$ vs. V, °°°$P < 0.001$; °°$P < 0.01$; °$P < 0.05$ vs 4 mA (post-hoc Bonferroni test).

cascades occurring within minutes of Ca2+ influx or receptor activation, as previously established in our laboratory (Cavalleri et al., 2018; Collo et al., 2018). Protein lysates were collected to assess the expression levels of pERK driven by Src-MEK activation, and the more downstream pP70-S6K, a specific substrate for mTOR activation (Fig. 4A). The results indicated that LF-LI ES effectively increased pERK and pP70-S6K as early as 1 min post-exposure (Fig. 4B and C). This rapid activation suggests a direct and immediate response of human DA neuronal cultures to LF-LI ES stimuli, implicating the ERK-mTOR pathway in the early phases of activity-dependent plasticity. These results, and particularly the second peak of pP70-S6K phosphorylation observed at 5 min, resemble very closely the delayed peak obtained with ketamine exposure (1 μM for 1h) in the same human DA neuronal cellular preparation (Cavalleri et al., 2018). The critical role of the ERK-Akt-mTOR phosphorylation cascade in neural plasticity induced by LF-LI ES was also confirmed by pre-treatments with the selective antagonists. At day 30 of differentiation, human DA neuron cultures were pretreated with selective phosphorylation inhibitors and receptor antagonists, including K252a (a TrkB receptor inhibitor), PP2 (a Src-family kinases inhibitor), LY294002 (a PI3K inhibitor) and Rapamycin (an mTOR inhibitor) (Fig. 4A). Following a 20-min pre-treatment with these inhibitors, the cultures were exposed to a 4 mA current for 1h, and 3 days later the human DA neuronal cultures were fixed with paraformaldehyde, immunostained with an anti-TH antibody and assessed morphologically for structural changes (Fig. 3D). Pre-treatment with K252a, PP2, LY294002, and Rapamycin all effectively blocked structural plasticity induced by LF-LI ES across all parameters. This suggests a critical role for the MEK-ERK signalling pathway in mediating the effects of LF-LI ES on DA neuron morphology and plasticity (Fig. 4E–G). Intriguingly, pretreatments with K252a, PP2, LY294002, and Rapamycin were also effective in inhibiting the plastic effects of Ketamine 1 μM 1h exposure on human DA neurons (Cavalleri et al., 2018), suggesting a mechanistic commonality.

3.4. *Structural plasticity induced by low frequency-low intensity electrical stimulation involves upregulation of D3 dopamine auto-receptor*

To further investigate the effects of LF-LI ES exposure on neural plasticity in human DA neurons, we quantified the mRNA expression of key neuronal genes associated to the control of DA neuron activity. These included TH as the rate-limiting synthetic enzyme for dopamine, the dopamine D2 auto-receptor (DA-D2R) and the dopamine D3 auto-receptor (DA-D3R) measured qPCR at multiple time points following LF-LI ES, i.e., 0, 6, 24, and 48h post-exposure. Gene expression analysis revealed a significant upregulation of DA-D3R mRNA at 6h. In contrast, the expression levels of TH and DA-D2R remained unchanged across all time points. Previously, we demonstrated that ketamine-induced structural plasticity in human DA neurons is mediated via a necessary concurrent activation of DA-D3R. Accordingly, exposure to the selective DA-D3R antagonist SB277011A was able to block the dendrite arborization outgrowth mediated by the ERK-mTOR pathways (Cavalleri et al., 2018). To test if DA-D3R viability was also necessary for LF-LI ES-induced neural plasticity, human DA neurons at day 30 of differentiation were pre-treated with SB277011A 20 min before LF-LI ES exposure. After 3 days, human DA neurons were fixed and immunostained using an anti-TH antibody to assess DA morphology and plasticity (Fig. 5B). Morphometric analysis indicated that pre-treatment with SB277011A significantly attenuated the plasticity-promoting effects of LF-LI ES on human DA neurons (Fig. 5C–E), supporting a key role for the DA-D3R in mediating structural plasticity also in an LF-LI ES protocol.

3.5. *Reversal of cortisol-induced neuroplasticity impairment in human DA neurons by low frequency-low intensity electrical stimulation in an in vitro depression model*

In a recent study, we demonstrated that sub-chronic exposure to cortisol, the primary stress hormone chronically increased in MDD patients (Cavalleri et al., 2024), significantly impairs dendritic plasticity in human iPSCs-derived DA neurons, and that 1 μM ketamine exposure for 1h effectively restores dendritic structures, reversing cortisol-induced damage (Cavalleri et al., 2024). Building upon these findings, we investigated the effects of 1h LF-LI ES on human DA neurons that were previously exposed to cortisol to inhibit neural plasticity mechanisms. In vitro cortisol 50 μM daily for 5 consecutive days reduce dendritic arborization and soma size in human DA neurons without affecting their survival (Cavalleri et al., 2024). These conditions were used in the present experiment, LF-LI ES being administered at 4 mA for either 1h or 2h on the 5th day following cortisol exposure (Fig. 6A). After 3 days without treatments, human DA neurons were fixed and immunostained using an anti-TH antibody to assess human DA neuron morphology and structural plasticity (Fig. 6B). Results showed a significantly LF-LI ES-dependent restoration to normal neuronal morphology in all parameters in cortisol-treated human DA neurons for both 1h and 2h LF-LI ES exposure (Fig. 6C).

4. Discussion

This study demonstrates that LF(2 Hz)-LI(2-4 mA) ES by biphasic electrical currents for a single 1h or 2h session promotes long term structural plasticity in human iPSC-derived DA neurons through calcium-dependent BDNF/TrkB and ERK-mTOR signaling. LF-LI ES also reversed cortisol-induced human DA neuron dendritic hypotrophy produced by sub-chronic cortisol exposure, a recent in vitro model that mimics the MDD endocrine liability, an effect similarly observed with ketamine (Cavalleri et al., 2024), thereby indicating a restorative potential of possible relevance for MDD pathophysiology. Importantly, these effects were observed in human neurons, representing a translational advance beyond traditional animal models. The similarities between the effects of LF-LI ES and ketamine are remarkable (Cavalleri et al., 2018). They both occur after 1h exposure, showing (a) enhanced dendrite length, branching, and soma size morphology; (b) temporal patterns of rapid molecular pathway activation within minutes after exposure, with increases of ERK phosphorylation occurring within 1 min and a bi-phasic p70-S6K phosphorylation profile with peak at 1 and 5 min; (c) dependence on calcium influx from voltage dependent L-type channels; (d) dependence on the BDNF/TrkB of stimulation-induced structural plasticity demonstrated using phosphorylation inhibitors targeting TrkB receptor, Src-kinase, PI3K, and mTOR (Cavalleri et al., 2018; Lin et al., 2021). Together, these data indicate convergence of LF-LI ES and ketamine onto a common mTOR-dependent neurotrophic signaling pathway, despite their distinct stimulus modalities, i.e., chemical vs. electrical, probably mediated by increased calcium influx (Li et al., 2010; Morton et al., 2013). Calcium influx through VGCC was essential for LF-LI ES-induced plasticity, aligning with findings that electrical fields modulate neuronal excitability via membrane depolarization (Babona-Pilipos et al., 2012; Diego-Santiago et al., 2025; Morton et al., 2013). This calcium dependency parallels ketamine's disinhibition-induced influx, underscoring calcium signaling as a key transducer for rapid antidepressant-associated plasticity via BDNF release (Li et al., 2010; Yang et al., 2020). The obligatory role of BDNF-TrkB signaling is in line with extensive literature demonstrating BDNF as a critical convergence point for antidepressant interventions and that deficient BDNF signaling characterizes depressive states (Castrén and Monteggia, 2021; Yang et al., 2020). Upregulation of DA-D3R mRNA 6h post LF-LI ES, and requirement for an active DA-D3R to drive LF-LI ES-induced structural plasticity in human DA neurons also align with previous ketamine studies. The selective increase in DA-D3R in the absence of changes in TH or DA-D2R expression is consistent with an adaptive response aimed at attenuating spontaneous dopaminergic activity while concurrently engaging neurotrophic pathways that support dendritic outgrowth (Morton et al., 2013). Accordingly, both ketamine and LF-LI ES effects on dendritic and soma growth were blocked by pre-treatment with selective DA-D3R antagonists, e.g., SB 277011A,

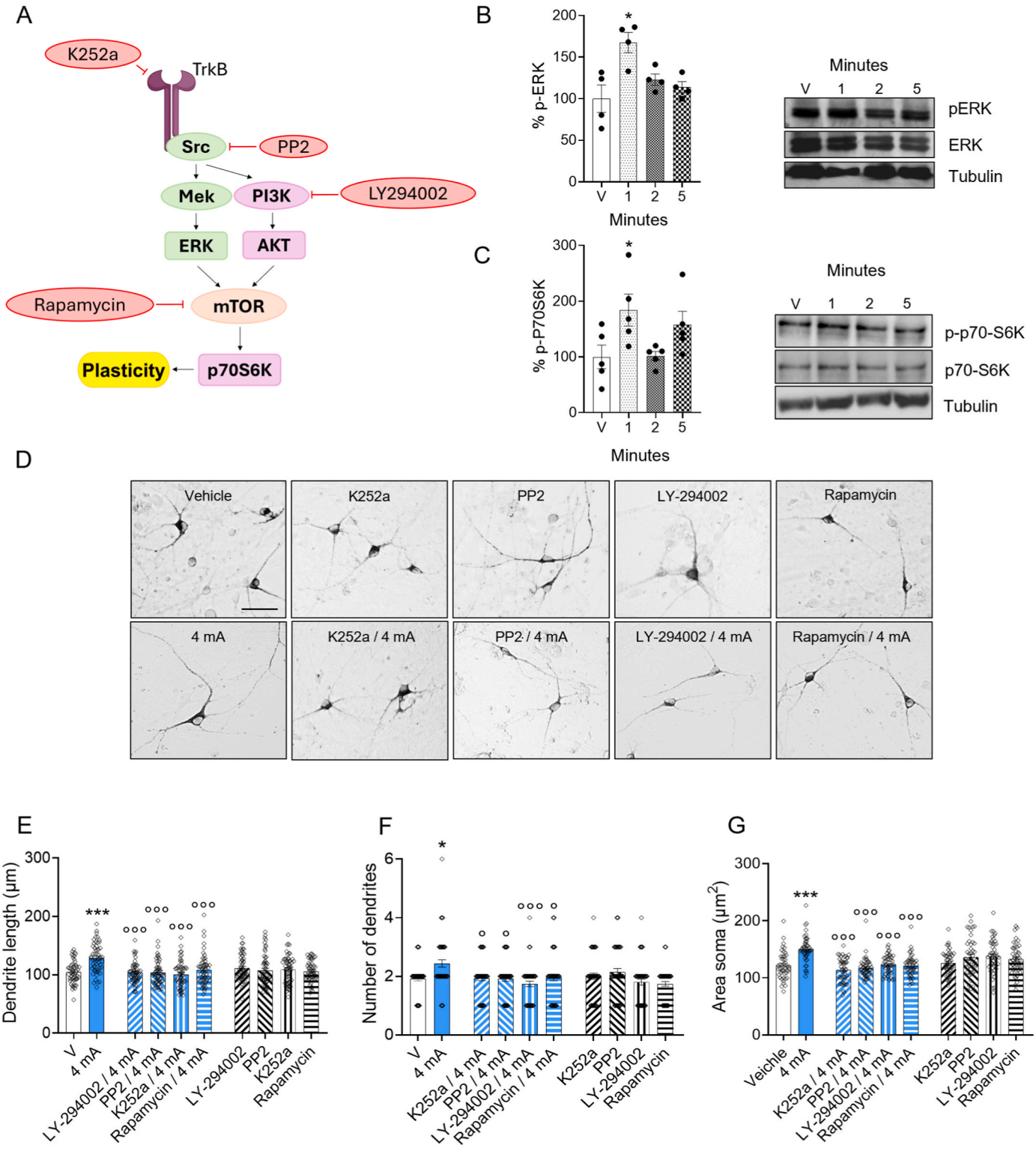

(caption on next page)

Fig. 4. Involvement of the BDNF-dependent ERK/mTOR pathway in neural plasticity induced by low-frequency low-intensity electrical stimulation. (A) Schematic representation of ERK/mTOR intracellular pathway and of the sites of actions of BDNF-TrkB signalling blockers used to explore their involvement in LF-LI ES-dependent neuroplasticity in human DA neuron cultures. (B-C) Effects of transient continuous exposure (1, 2 or 5 min) to LF-LI ES by a biphasic rectangular current of 4 mA amplitude on the p-ERK and p-p70-S6K levels measured with western blot and analysed by densitometry. Cultures were collected for immediately after the end of stimulation. p-ERK and p-p70-S6K levels were normalized to the corresponding ERK or p70-S6K and tubulin levels. The densitometric values are represented as a percentage of vehicle values (V). Friedman test showed an LF-LI ES exposure significant increase of p-ERK [Friedman statistic = 8,40, df = 3, p = 0.0190] and p-p70-S6K [Friedman statistic = 9.00, df = 3, p = 0.0196]. (D) Representative images showing morphological changes in human DA neurons exposed to a single LF-LI ES by a biphasic rectangular current of 4 mA amplitude for 1h and pretreated for 20 min with LY294002, PP2, K252a or rapamycin. Scale bar: 50 µm. (E-G) Quantification and statistical analysis using two-way ANOVA of (E) maximal dendrite length [interaction: $F(4,530) = 9.42$, $P < 0.001$; treatment factor: $F(1,530) = 0.45$, $P = 0.50$ ns; inhibition factor: $F(4,530) = 4.59$, $P < 0.01$], (F) number of primary dendrites [interaction: $F(4,490) = 4.13$, $P < 0.01$; treatment factor: $F(1,490) = 1.55$, $P = 0.21$ ns; inhibition factor: $F(4,490) = 4.91$, $P < 0.001$)] (full frequency distribution of dendrite counts per neuron shown in Supplementary Figure S4D), and (G) soma area [interaction: $F(4,440) = 15.28$, $P < 0.001$; treatment factor: $F(1,440) = 6.16$, $P < 0.05$; inhibition factor: $F(4,440) = 5.53$, $P < 0.001$] in human DA neurons. Individual data points represent single neuron measurements from two coverslips per group (technical replicate); each experiment was repeated at least twice independently. Data are presented as mean ± SEM. Statistical significance: ***P < 0.001; **P < 0.01; *P < 0.05 vs. V, °°°P < 0.001; °°P < 0.01; °P < 0.05 vs 4 mA (post-hoc Bonferroni test or Friedman test).

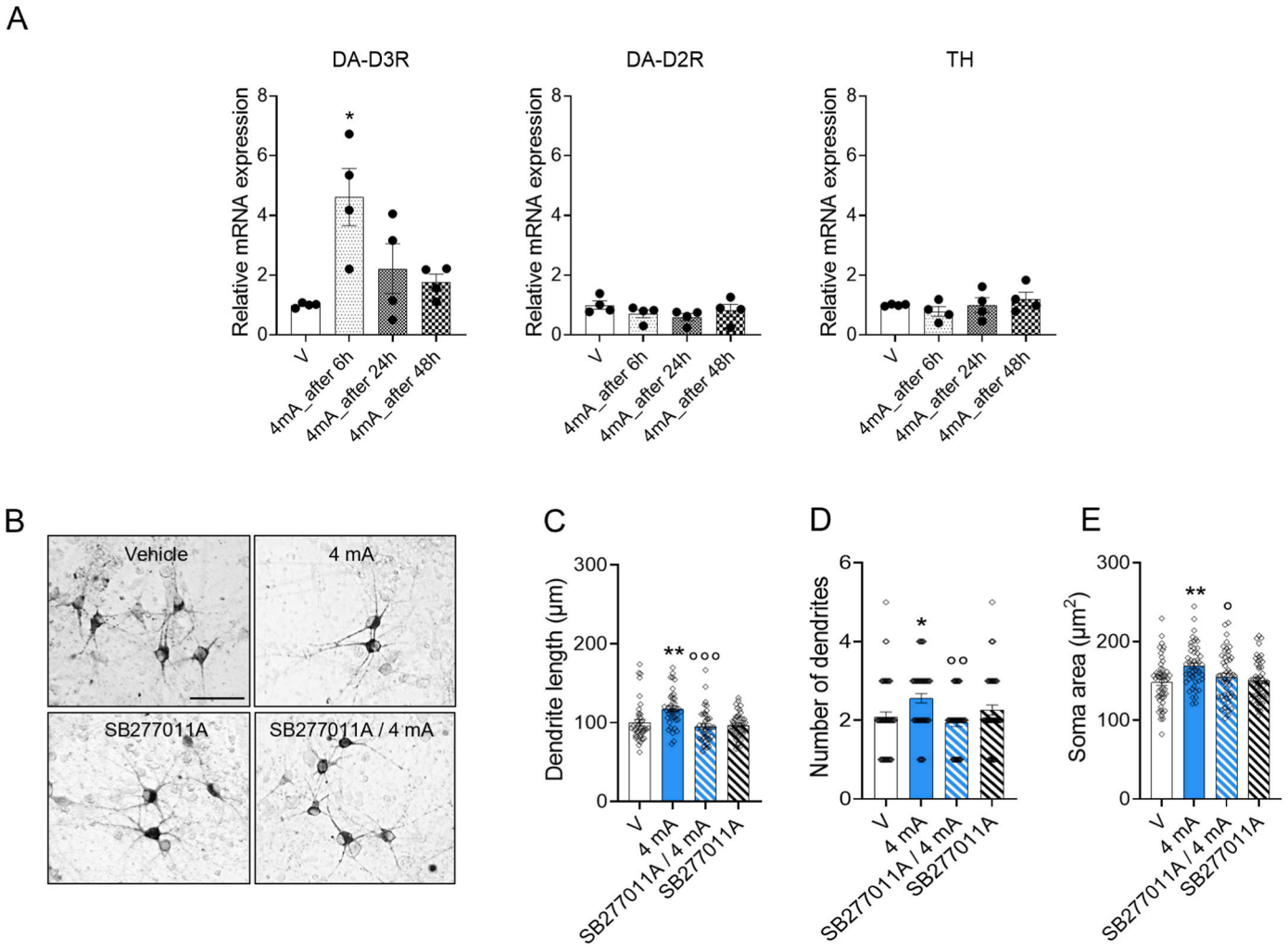

Fig. 5. Contribution of dopamine D3 auto-receptors to low-frequency low-intensity electrical stimulation-induced neural plasticity. (A) Gene expression analysis in human DA neurons following exposure to a 4 mA LF-LI ES for 1h, assessed at multiple time points (6, 24, or 48h post-stimulation). Relative gene expression quantification and statistical analysis at multiple time points vs V were performed using one-way ANOVA of TH [one-way ANOVA $F(3,12) = 0,84$, $P = 0.50$, ns,] DA-D2R [one-way ANOVA $F(3,12) = 1,21$, $P = 0.35$, ns] and DA-D3R [one-way ANOVA $F(3,12) = 5.77$, $P < 0.05$]. (B) Representative images showing morphological changes in human DA neurons exposed to a single LF-LI ES by biphasic electrical current of amplitude 4 mA for 1h and pretreated for 20 min with SB277011A. Scale bar: 50 µm. (C-E) Quantification and statistical analysis using two-way ANOVA of (C) maximal dendrite length [two-way ANOVA interaction: $F(1,160) = 8.03$, $P < 0.01$; treatment factor: $F(1,160) = 5.44$, $P < 0.05$; inhibition factor: $F(1,160) = 14.11$, $P < 0.001$], (D) number of primary dendrites [two-way ANOVA interaction: $F(1,196) = 11.33$, $P < 0.001$; treatment factor: $F(1,196) = 0.45$, $P = 0.50$ ns; inhibition factor: $F(1,196) = 3.43$, $P = 0.66$ ns] (full frequency distribution of dendrite counts per neuron shown in Supplementary Figure S4E), and (E) soma area [two-way ANOVA interaction: $F(1,195) = 4.77$, $P < 0.05$; treatment factor: $F(1,195) = 9.20$, $P < 0.01$; inhibition factor: $F(1,195) = 2.70$, $P = 0.10$ ns] in human DA neurons. Individual data points represent single neuron measurements from two coverslips per group (technical replicate); each experiment was repeated at least twice independently. Data are presented as mean ± SEM. Statistical significance: ***P < 0.001; **P < 0.01; *P < 0.05 vs. V, °°°P < 0.001; °°P < 0.01; °P < 0.05 vs 4 mA (post-hoc Bonferroni test).

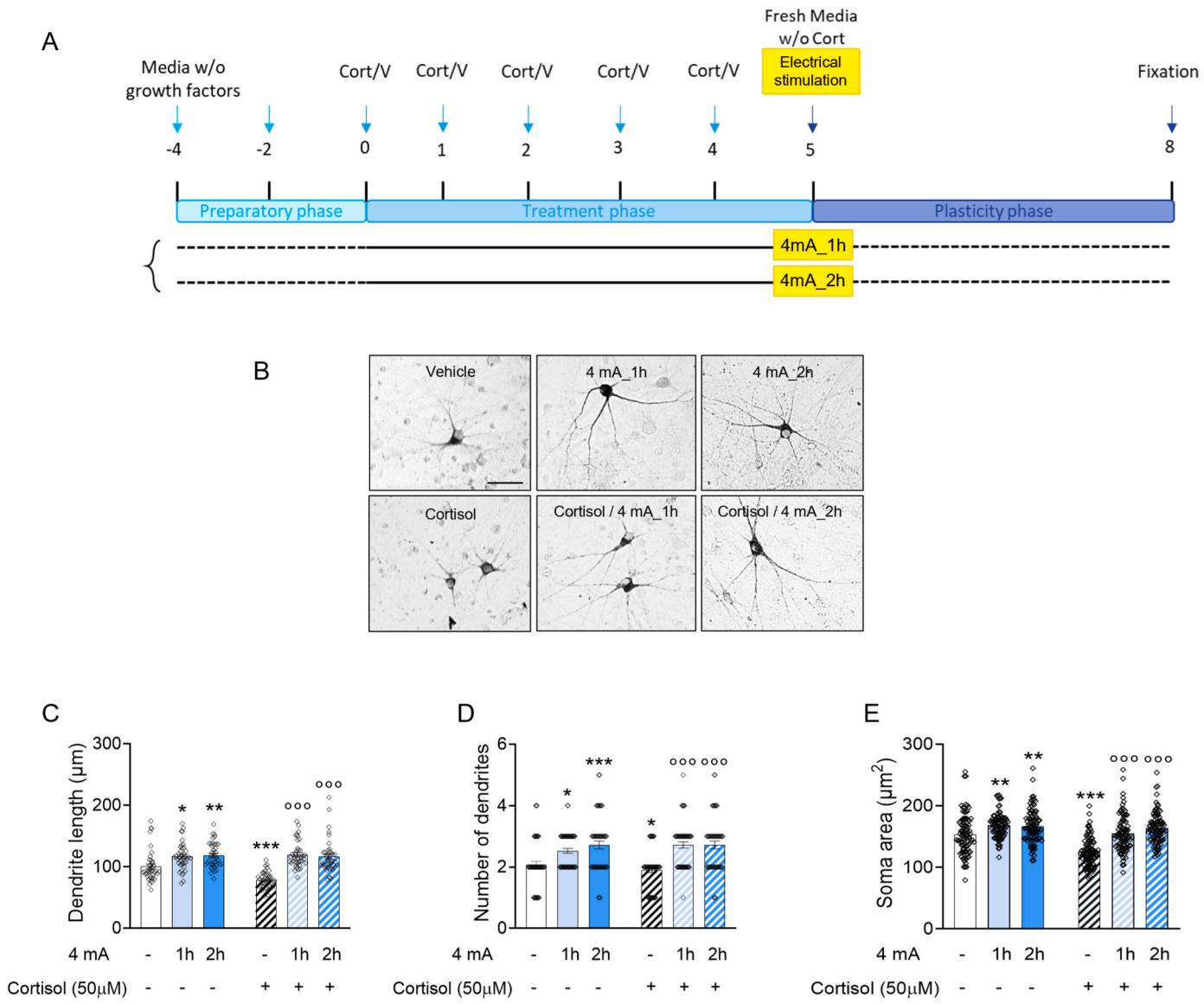

Fig. 6. Low-frequency low-intensity electrical stimulation-induced neuronal plasticity following sub-chronic exposures to high cortisol levels. (A) Schematic representation of the experimental protocol: cortisol (50 µM) was administered to human DA neuronal cultures for 5 days and LF-LI ES of 4 mA were performed for either 1 or 2h, starting 24h after last cortisol exposure (B) Representative images showing morphological changes in human DA neurons exposed to cortisol or vehicle and followed by 1 or 2h stimulation with an biphasic electrical current of amplitude 4 mA. Scale bar: 50 µm. (C-E) Quantification and statistical analysis using two-way ANOVA of (C) maximal dendrite length [interaction: $F(2,234) = 7.50$, $P < 0.001$; cortisol factor: $F(1,234) = 6.15$, $P < 0.05$; stimulation factor: $F(2,234) = 44.38$, $P < 0.001$], (D) number of primary dendrites [interaction $F(2,312) = 5.32$, $P < 0.01$; cortisol factor: $F(1,312) = 1.23$ $P = 0.2$ ns; stimulation factor: $F(2,312) = 42.66$, $P < 0.001$] (full frequency distribution of dendrite counts per neuron shown in Supplementary Figure S4F), and (E) soma area [interaction: $F(2,504) = 7.83$, $P < 0.001$; cortisol factor: $F(1,504) = 38.31$, $P < 0.001$; stimulation factor: $F(2,504) = 47.81$, $P < 0.001$] in human DA neurons. Individual data points represent single neuron measurements from two coverslips per group (technical replicate); each experiment was repeated at least twice independently. Data are presented as mean ± SEM. Statistical significance: ***$P < 0.001$; **$P < 0.01$; *$P < 0.05$ vs. V; °°°$P < 0.001$; °°$P < 0.01$; °$P < 0.05$ vs. cortisol (post-hoc Bonferroni test).

via a down-regulation of the mTOR pathway (Cavalleri et al., 2018; Collo et al., 2018). These effects were observed using an LF-LI ES with 4 mA biphasic current at 2 Hz for 1h or 2h single session exposure, parameters like those used in a protocol in primary hippocampal neurons of rats, showing that 1h/day exposure at 2 Hz boosts delta oscillation (1-4 Hz) (Leondopulos et al., 2012). Oscillatory rhythms in the brain create the context for encoding information and, at the same time, engage in adaptive structural and functional plastic processes aimed to optimize such encoding. The lower frequencies in the delta band are considered permissive for neuronal plasticity (Ousdal et al., 2022). Moreover, ventral tegmental area DA neurons have a propensity to show spontaneous intrinsic rhythmic activity in the 1–5 Hz range, both in vivo and in vitro. In a recent optogenetic study in mouse brain slices, mesencephalic DA neurons of the ventral tegmental area showed resonance spectra to laser pulses peaking at 1-2 Hz frequency (van der Velden et al., 2020). It is tempting to suggest that the 2 Hz stimuli implemented in the present LF-LI ES protocol would have acted on this predisposed resonant substrate of the DA neuron, enhancing neural activity and triggering neurotrophic pathway phosphorylation to provide an adaptive structural support to the enhanced function. Intriguingly, the LF-LI ES current amplitude and exposure time match or overlap some effective neuromodulation therapies. For example, tDCS and tACS protocols with demonstrated clinical efficacy typically use 1-2 mA currents over 20-30 min at 0 Hz (tDCS) or 6-10 Hz (tACS), respectively (Ren

et al., 2025), inducing acute and longer-term BDNF expression and structural plasticity changes in local cortical neurons and in distant limbic circuit structures (Brunoni et al., 2016, 2017; Korai et al., 2021), including the mesocorticolimbic DA system of mice and humans (De Paolis et al., 2025; Fonteneau et al., 2018). Low-frequency (0-20 Hz) DBS protocols have been rarely used in humans, but these studies show efficacy in TRD patients not different from high frequency (130-185 Hz) DBS protocols (Figee et al., 2022). The DBS electrodes are often implanted in subcortical targets that include ascending projections from mesencephalic DA neurons, e.g., nucleus accumbens and medial forebrain bundle (Figee et al., 2022). Rodent studies showed that these placements of DBS electrodes increased DA neurons phasic and tonic activity, dopamine release, BDNF expression, oxidative phosphorylation and functional connectivity (Li et al., 2023; Miguel Telega et al., 2025). These results are in line with long-standing evidence that somatodendritic low frequency stimulations of DA neurons were shown to release dopamine in rodents (Rice et al. 1997, 2011). These DA neuron-specific findings suggest that a new technology capable of reaching the ventral mesencephalon and delivering biphasic 2 Hz LF-LI ES could possibly ameliorate motivational symptoms of TRD via dopamine release and enhanced long-term structural neuroplasticity rather than transient modulatory effects of neural activity or dopamine release probably requiring repeated exposure sessions, e.g., biweekly, to maintain the therapeutic effect. Interventions converging on DA circuit plasticity may complement frontocortical glutamatergic strategies, in particular pharmacological treatments. For example, both ketamine and the DA-D3R agonists like pramipexole exhibit antidepressant effects and promote structural plasticity via BDNF-mTOR signaling in human DA neurons (Collo et al., 2018). The convergent effects of pharmacological (ketamine, D3 agonists) and physical (LF-LI ES) interventions on mesencephalic DA neuronal plasticity may benefit TRD patients subtype characterized by severe anhedonia. Limitations of present work include in vitro simplifications lacking network complexity and in vivo modulation dynamics. The two-dimensional culture system only partially replicates circuit-level interactions, glial influences, or neuromodulatory inputs present in vivo. Future work should address three-dimensional human organoid models. Detailed biophysical characterization of applied currents and field distributions vs. neuronal plasticity propensity, and logistics solution for electrode placement in vivo are necessary steps towards translational relevance (Babona-Pilipos et al., 2012).

In conclusion, LF-LI ES by biphasic electrical currents induces molecular and structural plasticity akin to ketamine in human DA neurons and reverses cortisol-induced dendrite arborization hypotrophy, supporting its potential as a possible neuromodulatory antidepressant strategy. This aligns with clinical neuromodulation's emerging role and encourages further technological optimization. Understanding convergent mechanisms between pharmacological and electrical interventions may enable personalized treatment strategies optimizing plasticity induction while minimizing adverse effects.

Author disclosure

This work was supported by Grant from ex 60% University of Brescia to Ginetta Collo. The funding source had no involvement in study design, data collection, analysis and interpretation, writing of the report, or the decision to submit the article for publication.

CRediT authorship contribution statement

Giulia Sofia Marcotto: Data curation, Formal analysis, Investigation, Writing – original draft. **Michela Borghetti:** Formal analysis, Methodology. **Jonida Bitraj:** Investigation. **Laura Cavalleri:** Formal analysis, Investigation. **Mauro Serpelloni:** Conceptualization, Writing – review & editing. **Michele Zoli:** Writing – review & editing. **Maurizio Memo:** Conceptualization, Writing – review & editing. **Emilio Sardini:** Conceptualization, Supervision. **Ginetta Collo:** Conceptualization, Formal analysis, Funding acquisition, Methodology, Supervision, Writing – original draft, Writing – review & editing.

Declaration of competing interest

The authors declare that they have no known competing financial interests or personal relationships that could have appeared to influence the work reported in this paper.

ABBREVIATIONS

BDNF	brain-derived neurotrophic factor
BDS	deep brain stimulation
BSA	bovine serum albumin
DA	dopaminergic
DAB	3,3′diaminobenzidine
DA-D2R	dopamine D2 auto-receptor
DA-D3R	dopamine D3 auto-receptor
ECT	electro convulsive therapy
ERK	extracellular signal-regulated kinase
ES	electrical stimulation
GABA	gamma-aminobutyric acid
GAPDH	Glyceraldehyde-3-phosphate dehydrogenase
iPSCs	induced pluripotent stem cells
LF-LI ES	Low-frequency low-intensity electrical stimulation
MDD	Major Depressive Disorders
mTOR	mammalian target of rapamycin
NGS	normal goat serum
NMDA	N-methyl-D-aspartate
NPCs	neural progenitor cells
ON	overnight
PI3K	phosphoinositide 3-kinase
qPCR	quantitative PCR
RIPA	radioimmunoprecipitation assay
RT	room temperature
tACS	transcranial alternate current stimulation
tDCS	transcranial direct current stimulation
TH	tyrosine hydroxylase
TRD	treatment resistant depression
TrkB	tropomyosin receptor kinase B
VGCCs	voltage-gated calcium channels

Appendix A. Supplementary data

Supplementary data to this article can be found online at https://doi.org/10.1016/j.neuropharm.2026.110964.

Data availability

The data supporting the findings of this study are available within the article. Data for individual data points are available from the corresponding author upon reasonable request.

References

American Psychiatric Association, 2022. Diagnostic and Statistical Manual of Mental Disorders. Diagnostic and Statistical Manual of Mental Disorders. https://doi.org/10.1176/appi.books.9780890425787.

Babona-Pilipos, R., Pritchard-Oh, A., Popovic, M.R., Morshead, C.M., 2012. Biphasic monopolar electrical stimulation induces rapid and directed galvanotaxis in adult subependymal neural precursors. https://doi.org/10.1186/s13287-015-0049-6.

Balbinot, G., Milosevic, M., Morshead, C.M., Iwasa, S.N., Zariffa, J., Milosevic, L., Valiante, T.A., Hoffer, J.A., Popovic, M.R., 2025. The mechanisms of electrical neuromodulation. J. Physiol. 603, 247–284. https://doi.org/10.1113/JP286205.

Berman, R.M., Cappiello, A., Anand, A., Oren, D.A., Heninger, G.R., Charney, D.S., Krystal, J.H., 2000. Antidepressant effects of ketamine in depressed patients. Biol. Psychiatry 47, 351–354. https://doi.org/10.1016/S0006-3223(99)00230-9.

Bertucci, C., Koppes, R., Dumont, C., Koppes, A., 2019. Neural responses to electrical stimulation in 2D and 3D in vitro environments. Brain Res. Bull. 152, 265–284. https://doi.org/10.1016/j.brainresbull.2019.07.016.

Brunoni, A.R., Chaimani, A., Moffa, A.H., Razza, L.B., Gattaz, W.F., Daskalakis, Z.J., Carvalho, A.F., 2017. Repetitive transcranial magnetic stimulation for the acute treatment of major depressive episodes: a systematic review with network meta-analysis. JAMA Psychiatry 74, 143–152. https://doi.org/10.1001/jamapsychiatry.2016.3644.

Brunoni, A.R., Tortella, G., Benseñor, I.M., Lotufo, P.A., Carvalho, A.F., Fregni, F., 2016. Cognitive effects of transcranial direct current stimulation in depression: results from the SELECT-TDCS trial and insights for further clinical trials. J. Affect. Disord. 202, 46–52. https://doi.org/10.1016/j.jad.2016.03.066.

Castrén, E., Monteggia, L.M., 2021. Brain-derived neurotrophic factor signaling in depression and antidepressant action. Biol. Psychiatry 90, 128–136. https://doi.org/10.1016/j.biopsych.2021.05.008.

Cavalleri, L., Dassieni, I., Marcotto, G.S., Zoli, M., Merlo Pich, E., Collo, G., 2024. Cortisol-dependent impairment of dendrite plasticity in human dopaminergic neurons derived from hiPSCs is restored by ketamine: relevance for major depressive disorders. Neurosci. Appl. 3. https://doi.org/10.1016/j.nsa.2024.104049.

Cavalleri, L., Merlo Pich, E., Millan, M.J., Chiamulera, C., Kunath, T., Spano, P.F., Collo, G., 2018. Ketamine enhances structural plasticity in mouse mesencephalic and human iPSC-derived dopaminergic neurons via AMPAR-driven BDNF and mTOR signaling. Mol. Psychiatr. 23, 812–823. https://doi.org/10.1038/mp.2017.241.

Collo, G., Cavalleri, L., Bono, F., Mora, C., Fedele, S., Invernizzi, R.W., Gennarelli, M., Piovani, G., Kunath, T., Millan, M.J., Merlo Pich, E., Spano, P., 2018. Ropinirole and pramipexole promote structural plasticity in human iPSC-Derived dopaminergic neurons via BDNF and mTOR signaling. Neural Plast. https://doi.org/10.1155/2018/4196961, 2018.

De Paolis, M.L., Loffredo, G., Krashia, P., La Barbera, L., Nobili, A., Cauzzi, E., Babicola, L., Di Segni, M., Coccurello, R., Puglisi-Allegra, S., Latagliata, E.C., D'Amelio, M., 2025. Repetitive prefrontal tDCS activates VTA dopaminergic neurons, resulting in attenuation of Alzheimer's disease-like deficits in Tg2576 mice. Alzheimers Res. Ther. 17, 94. https://doi.org/10.1186/s13195-025-01736-4.

Diego-Santiago, M. del P., González, M.U., Zamora Sánchez, E.M., Cortes-Carrillo, N., Dotti, C., Guix, F.X., Mobini, S., 2025. Bioelectric stimulation outperforms brain derived neurotrophic factor in promoting neuronal maturation. Sci. Rep. 15 (1 15), 4772. https://doi.org/10.1038/s41598-025-89330-4, 2025.

Dukart, J., Regen, F., Kherif, F., Colla, M., Bajbouj, M., Heuser, I., Frackowiak, R.S., Draganski, B., 2014. Electroconvulsive therapy-induced brain plasticity determines therapeutic outcome in mood disorders. Proc. Natl. Acad. Sci. U. S. A. 111, 1156–1161. https://doi.org/10.1073/pnas.1321399111.

Fava, M., 2003. Diagnosis and definition of treatment-resistant depression. Biol. Psychiatry 53, 649–659. https://doi.org/10.1016/S0006-3223(03)00231-2.

Fedele, S., Collo, G., Behr, K., Bischofberger, J., Müller, S., Kunath, T., Christensen, K., Gündner, A.L., Graf, M., Jagasia, R., Taylor, V., 2017. Expansion of human midbrain floor plate progenitors from induced pluripotent stem cells increases dopaminergic neuron differentiation potential. Sci. Rep. 7. https://doi.org/10.1038/s41598-017-05633-1.

Figee, M., Riva-Posse, P., Choi, K.S., Bederson, L., Mayberg, H.S., Kopell, B.H., 2022. Deep brain stimulation for depression. Neurotherapeutics 19, 1229–1245. https://doi.org/10.1007/s13311-022-01270-3.

Fonteneau, C., Redoute, J., Haesebaert, F., Le Bars, D., Costes, N., Suaud-Chagny, M.F., Brunelin, J., 2018. Frontal transcranial direct current stimulation induces dopamine release in the ventral striatum in human. Cerebr. Cortex 28, 2636–2646. https://doi.org/10.1093/cercor/bhy093.

Herrington, T.M., Cheng, J.J., Eskandar, E.N., 2016. Mechanisms of deep brain stimulation. J. Neurophysiol. 115, 19–38. https://doi.org/10.1152/jn.00281.2015.

Kobelt, L.J., Wilkinson, A.E., McCormick, A.M., Willits, R.K., Leipzig, N.D., 2014. Short duration electrical stimulation to enhance neurite outgrowth and maturation of adult neural stem progenitor cells. Ann. Biomed. Eng. 42, 2164–2176. https://doi.org/10.1007/s10439-014-1058-9.

Korai, S.A., Ranieri, F., Di Lazzaro, V., Papa, M., Cirillo, G., 2021. Neurobiological after-effects of low intensity transcranial electric stimulation of the human nervous system: from basic mechanisms to metaplasticity. Front. Neurol. 12, 587771. https://doi.org/10.3389/fneur.2021.587771.

Kriks, S., Shim, J.W., Piao, J., Ganat, Y.M., Wakeman, D.R., Xie, Z., Carrillo-Reid, L., Auyeung, G., Antonacci, C., Buch, A., Yang, L., Beal, M.F., Surmeier, D.J., Kordower, J.H., Tabar, V., Studer, L., 2011. Dopamine neurons derived from human ES cells efficiently engraft in animal models of Parkinson's disease. Nature 480, 547–551. https://doi.org/10.1038/nature10648.

Lee, W.H., Lisanby, S.H., Laine, A.F., Peterchev, A.V., 2016. Comparison of electric field strength and spatial distribution of electroconvulsive therapy and magnetic seizure therapy in a realistic human head model. Eur. Psychiatry 36, 55–64. https://doi.org/10.1016/j.eurpsy.2016.03.003.

Leondopulos, S.S., Boehler, M.D., Wheeler, B.C., Brewer, G.J., 2012. Chronic stimulation of cultured neuronal networks boosts low-frequency oscillatory activity at theta and gamma with spikes phase-locked to gamma frequencies. J. Neural. Eng. 9. https://doi.org/10.1088/1741-2560/9/2/026015.

Li, N., Lee, B., Liu, R.J., Banasr, M., Dwyer, J.M., Iwata, M., Li, X.Y., Aghajanian, G., Duman, R.S., 2010. mTOR-dependent synapse formation underlies the rapid antidepressant effects of NMDA antagonists. Science 329, 959–964. https://doi.org/10.1126/science.1190287.

Li, S.J., Lo, Y.C., Tseng, H.Y., Lin, S.H., Kuo, C.H., Chen, T.C., Chang, C.W., Liang, Y.W., Lin, Y.C., Wang, C.Y., Cho, T.Y., Wang, M.H., Chen, C. Te, Chen, Y.Y., 2023. Nucleus accumbens deep brain stimulation improves depressive-like behaviors through BDNF-mediated alterations in brain functional connectivity of dopaminergic pathway. Neurobiol. Stress 26. https://doi.org/10.1016/j.ynstr.2023.100566.

Limousin, P., Foltynie, T., 2019. Long-term outcomes of deep brain stimulation in Parkinson disease. Nat. Rev. Neurol. 15, 234–242. https://doi.org/10.1038/s41582-019-0145-9.

Lin, P.Y., Ma, Z.Z., Mahgoub, M., Kavalali, E.T., Monteggia, L.M., 2021. A synaptic locus for TrkB signaling underlying ketamine rapid antidepressant action. Cell Rep. 36, 109513. https://doi.org/10.1016/j.celrep.2021.109513.

Lozano, A.M., Giacobbe, P., Hamani, C., Rizvi, S.J., Kennedy, S.H., Kolivakis, T.T., Debonnel, G., Sadikot, A.F., Lam, R.W., Howard, A.K., Ilcewicz-Klimek, M., Honey, C.R., Mayberg, H.S., 2012. A multicenter pilot study of subcallosal cingulate area deep brain stimulation for treatment-resistant depression. J. Neurosurg. 116, 315–322. https://doi.org/10.3171/2011.10.JNS102122.

Malhi, G.S., Mann, J.J., 2018. Depression. Lancet 392, 2299–2312. https://doi.org/10.1016/S0140-6736(18)31948-2.

Maruyama, T., Kanaji, T., Nakade, S., Kanno, T., Mikoshiba, K., 1997. 2APB, 2-aminoethoxydiphenyl borate, a membrane-penetrable modulator of Ins(1,4,5)P3-induced Ca2+ release. J. Biochem. 122 (3), 498–505. https://doi.org/10.1093/oxfordjournals.jbchem.a021780.

Mayberg, H.S., Lozano, A.M., Voon, V., McNeely, H.E., Seminowicz, D., Hamani, C., Schwalb, J.M., Kennedy, S.H., 2005. Deep brain stimulation for treatment-resistant depression. Neuron 45, 651–660. https://doi.org/10.1016/j.neuron.2005.02.014.

McCracken, C.B., Grace, A.A., 2007. High-frequency deep brain stimulation of the nucleus accumbens region suppresses neuronal activity and selectively modulates afferent drive in rat orbitofrontal cortex in vivo. J. Neurosci. 27, 12601–12610. https://doi.org/10.1523/JNEUROSCI.3750-07.2007.

Miguel Telega, L., Ashouri Vajari, D., Ramanathan, C., Coenen, V.A., Döbrössy, M.D., 2025. Chronic in vivo sequelae of repetitive acute mfb-DBS on accumbal dopamine and midbrain neuronal activity. J. Neurochem. 169. https://doi.org/10.1111/jnc.16223.

Morton, R.A., Norlin, M.S., Vollmer, C.C., Valenzuela, C.F., 2013. Characterization of L-type voltage-gated Ca2+ channel expression and function in developing CA3 pyramidal neurons. Neuroscience 238, 59–70. https://doi.org/10.1016/j.neuroscience.2013.02.008.

Nestler, E.J., Carlezon, W.A., 2006. The mesolimbic dopamine reward circuit in depression. Biol. Psychiatry 59, 1151–1159. https://doi.org/10.1016/j.biopsych.2005.09.018.

Ousdal, O.T., Brancati, G.E., Kessler, U., Erchinger, V., Dale, A.M., Abbott, C., Oltedal, L., 2022. The neurobiological effects of electroconvulsive therapy studied through magnetic resonance: what have we learned, and where do we go? Biol. Psychiatry 91, 540–549. https://doi.org/10.1016/j.biopsych.2021.05.023.

Pirnia, T., Joshi, S.H., Leaver, A.M., Vasavada, M., Njau, S., Woods, R.P., Espinoza, R., Narr, K.L., 2016. Electroconvulsive therapy and structural neuroplasticity in neocortical, limbic and paralimbic cortex. Transl. Psychiatry 6. https://doi.org/10.1038/tp.2016.102.

Pizzagalli, D.A., 2014. Depression, stress, and anhedonia: toward a synthesis and integrated model. Annu. Rev. Clin. Psychol. 10, 393–423. https://doi.org/10.1146/annurev-clinpsy-050212-185606.

Polyakova, M., Schroeter, M.L., Elzinga, B.M., Holiga, S., Schoenknecht, P., De Kloet, E. R., Molendijk, M.L., 2015. Brain-derived neurotrophic factor and antidepressive effect of electroconvulsive therapy: systematic review and meta-analyses of the preclinical and clinical literature. PLoS One 10, e0141564. https://doi.org/10.1371/journal.pone.0141564.

Ramasubbu, R., Lang, S., Kiss, Z.H.T., 2018. Dosing of electrical parameters in deep brain stimulation (DBS) for intractable depression: a review of clinical studies. Front. Psychiatr. 9. https://doi.org/10.3389/fpsyt.2018.00302.

Ren, C., Pagali, S.R., Wang, Z., Kung, S., Boyapati, R.B., Islam, K., Li, J.W., Shelton, K.M., Waniger, A., Rydberg, A.M., Hassett, L.C., Croarkin, P.E., Lundstrom, B.N., Pascual-Leone, A., Lapid, M.I., 2025. Transcranial electrical stimulation in treatment of depression: a systematic review and meta-analysis. JAMA Netw. Open 8. https://doi.org/10.1001/jamanetworkopen.2025.16459.

Rice, M.E., Cragg, S.J., Greenfield, S.A., 1997. Characteristics of electrically evoked somatodendritic dopamine release in substantia nigra and ventral tegmental area in vitro. J. Neurophysiol. 77, 853–862. https://doi.org/10.1152/jn.1997.77.2.853.

Rice, M.E., Patel, J.C., Cragg, S.J., 2011. Dopamine release in the basal ganglia. Neuroscience 198, 112–137. https://doi.org/10.1016/j.neuroscience.2011.08.066.

Schmidt, U., Beyer, C., Oestreicher, A.B., Reisert, I., Schilling, K., Pilgrim, C., 1996. Activation of dopaminergic D1 receptors promotes morphogenesis of developing striatal neurons. Neuroscience 74, 453–460. https://doi.org/10.1016/0306-4522(96)00201-1.

Sorri, A., Järventausta, K., Kampman, O., Lehtimäki, K., Björkqvist, M., Tuohimaa, K., Hämäläinen, M., Moilanen, E., Leinonen, E., 2018. Effect of electroconvulsive therapy on brain-derived neurotrophic factor levels in patients with major depressive disorder. Brain Behav. 8. https://doi.org/10.1002/brb3.1101.

Strong, C.E., Kabbaj, M., 2018. On the safety of repeated ketamine infusions for the treatment of depression: Effects of sex and developmental periods. Neurobiol. Stress 9, 166–175. https://doi.org/10.1016/j.ynstr.2018.09.001.

Tang-Schomer, M.D., 2018. 3D axon growth by exogenous electrical stimulus and soluble factors. Brain Res. 1678, 288–296. https://doi.org/10.1016/j.brainres.2017.10.032.

Tominami, K., Kudo, T.A., Noguchi, T., Hayashi, Y., Luo, Y.R., Tanaka, T., Matsushita, A., Izumi, S., Sato, H., Gengyo-Ando, K., Matsuzawa, A., Hong, G., Nakai, J., 2024. Physical stimulation methods developed for in vitro neuronal differentiation studies of PC12 cells: a comprehensive review. Int. J. Mol. Sci. 25. https://doi.org/10.3390/ijms25020772.

van der Velden, L., Vinck, M.A., Wadman, W.J., 2020. Resonance in the mouse ventral tegmental area dopaminergic network induced by regular and poisson distributed

optogenetic stimulation in-vitro. Front. Comput. Neurosci. 14. https://doi.org/10.3389/fncom.2020.00011.

Wang, M., Li, P., Liu, M., Song, W., Wu, Q., Fan, Y., 2013. Potential protective effect of biphasic electrical stimulation against growth factor-deprived apoptosis on olfactory bulb neural progenitor cells through the brain-derived neurotrophic factor-phosphatidylinositol 3′-kinase/Akt pathway. Exp. Biol. Med. 238, 951–959. https://doi.org/10.1177/1535370213494635.

Wang, S., Guan, S., Sun, C., Liu, H., Liu, T., Ma, X., 2023. Electrical stimulation enhances the neuronal differentiation of neural stem cells in three-dimensional conductive scaffolds through the voltage-gated calcium ion channel. Brain Res. 1798. https://doi.org/10.1016/j.brainres.2022.148163.

Yang, T., Nie, Z., Shu, H., Kuang, Y., Chen, X., Cheng, J., Yu, S., Liu, H., 2020. The role of BDNF on neural plasticity in depression. Front. Cell. Neurosci. 14, 82. https://doi.org/10.3389/fncel.2020.00082.

Zarate, C.A., Singh, J.B., Carlson, P.J., Brutsche, N.E., Ameli, R., Luckenbaugh, D.A., Charney, D.S., Manji, H.K., 2006. A randomized trial of an N-methyl-D-aspartate antagonist in treatment-resistant major depression. Arch. Gen. Psychiatry 63, 856–864. https://doi.org/10.1001/archpsyc.63.8.856.

Zhu, R., Sun, Z., Li, C., Ramakrishna, S., Chiu, K., He, L., 2019. Electrical stimulation affects neural stem cell fate and function in vitro. Exp. Neurol. 319. https://doi.org/10.1016/j.expneurol.2019.112963.